

# A-dependence of the $\gamma$ - and p-induced production of the $\Lambda(1520)$ from nuclei

M. Kaskulov<sup>1,a</sup>, L. Roca<sup>2,b</sup>, and E. Oset<sup>1,c</sup>

<sup>1</sup> Departamento de Física Teórica and IFIC, Centro Mixto Universidad de Valencia-CSIC, Institutos de Investigación de Paterna, Aptd. 22085, 46071 Valencia, Spain

<sup>2</sup> Departamento de Física, Universidad de Murcia, E-30100 Murcia, Spain

Received: 31 January 2006 / Revised: 6 April 2006 /  
Published online: 22 June 2006 – © Società Italiana di Fisica / Springer-Verlag 2006  
Communicated by A. Molinari

**Abstract.** Using results of a recent calculation of the  $\Lambda(1520)$  in the nuclear medium, which show that the medium width is about five times the free width, we study the  $A$ -dependence of the  $\Lambda(1520)$  production cross-section in the reactions  $\gamma A \rightarrow K^+ \Lambda(1520) A'$  and  $p A \rightarrow p K^+ \Lambda(1520) A'$ . We find a sizable  $A$ -dependence in the ratio of the nuclear cross-sections for heavy nuclei with respect to a light one due to the large value of the  $\Lambda(1520)$  width in the medium, showing that devoted experiments, easily within reach in present facilities, can provide good information on that magnitude by measuring the cross-sections studied here.

**PACS.** 21.80.+a Hypernuclei – 21.65.+f Nuclear matter

## 1 Introduction

The renormalization of particle properties in nuclei is a topic that captures permanent attention. Devoted many-body calculations are done in order to evaluate these properties and parallelly there are experimental searches to test these theoretical predictions, while other times it goes the other way around, with first observation of drastic changes in the nuclear medium. One of the simplest cases from the experimental point of view is the renormalization of the  $\Delta(1232)$ -resonance which can be seen in numerous reactions, but perhaps best in the total photonuclear cross-section [1]. With this experiment one could test theoretical predictions made in [2] for the  $\Delta$  self-energy and the calculations of the photonuclear cross-section were done in [3]. One might guess then that other resonances could be tested so easily by means of total photoproduction, but the  $\Delta$  is maybe an exceptional case where the total cross-section is absolutely dominated by  $\Delta$  excitation in its range of energies. This method would obviously not work to test resonances with strangeness where other particles with strangeness will have to be detected in coincidence, which will most probably be distorted in the nucleus blurring the signals for genuine changes of the resonance in the nucleus. Other times the production cross-section will

be a very small fraction of the total cross-section and pose different but equally difficult problems. Yet, the determination of these properties bears much information on the dynamics of the hadron interaction and the efforts to find out these properties are fully justified.

One of the interesting cases of medium renormalization is that of the  $\phi$ -meson where theories predict an increase of the width in nuclear matter of the order of a factor five to ten [4–6]. Yet, the experimental observation of the change in the width in  $\phi$  photonuclear production is impractical if one looks for a broadening of the mass distribution of the  $\phi$  decay products ( $K\bar{K}$ ) for slow  $\phi$ 's, as guessed from [7] and further elaborated in [8].

One step forward in this direction was given in the experiment [9] where the  $A$ -dependence of the cross-section was studied and from there sizable changes of the  $\phi$  width in the nuclear medium were determined. Stimulated by this experiment a calculation was done in ref. [10] by using the theoretical values of this magnitude found in [4–6] which indeed lead to a marked  $A$ -dependence, although discrepancies of the theory and experiment remain that require further thoughts. The success of the method led to calculations of the  $A$ -dependence in the proton-induced  $\phi$  production in nuclei, showing theoretically that the method is well suited to determine changes of the  $\phi$  width in the medium [11]. Successively, an experimental proposal to carry out this experiment was approved in the COSY facility at Juelich [12].

<sup>a</sup> e-mail: kaskulov@ific.uv.es

<sup>b</sup> e-mail: luisroca@um.es

<sup>c</sup> e-mail: oset@ific.uv.es

One of the other resonances recently found theoretically with a spectacular change of the width in the medium is the  $\Lambda(1520)$ . This resonance could qualify as a dynamically generated resonance from the collaboration of the  $\pi\Sigma^*(1385)$ ,  $\bar{K}N$  and  $\pi\Sigma$  channels [13–15] and these channels get largely renormalized in the nucleus [16]. One of them is easily visualized: the coupling of  $\Lambda(1520)$  to  $\pi\Sigma^*(1385)$  is quite large, but the width in vacuum into this channel is extremely small since there is only phase space for the decay through the width of the  $\Sigma^*(1385)$ . However, in the nucleus the pion can become a  $ph$  and automatically there is plenty of phase space for the decay. This source alone leads to a width in the medium as large as the free width. The renormalization of the other channels also leads to large corrections and finally the total width at normal nuclear-matter density turns out to be as big as five times the free width. Such a spectacular change should be clearly observable and the purpose of the present work is to present a method of analysis based on two reactions, exploiting the  $A$ -dependence of the cross-section. The two reactions are the photonuclear excitation and the proton-induced production of the  $\Lambda(1520)$ . As we shall see, in both reactions one predicts a strong  $A$ -dependence which is amenable to experimental observation in present experimental facilities.

## 2 The $\Lambda(1520)$ in the nuclear medium

In the description of the  $\Lambda(1520)$  properties in the nuclear medium we closely follow the formalism developed in ref. [16]. Here, we briefly summarize the main results of that study.

In the nuclear medium the  $\Lambda(1520)$  gets renormalized through the conventional  $d$ -wave decay channels including  $\Lambda(1520) \rightarrow \bar{K}N$  and  $\Lambda(1520) \rightarrow \pi\Sigma$  which account for practically all of the  $\Lambda(1520)$  free width  $\Gamma_{free} \simeq 15.6$  MeV [17]. In addition in ref. [16], as a novel element, the  $s$ -wave decay  $\Lambda(1520) \rightarrow \pi\Sigma^*(1385)$  has been considered, which is forbidden in the free space for the nominal masses of the  $\Lambda(1520)$  and  $\Sigma^*(1385)$  but opens in the nuclear medium because of an additional phase space available for the decay products. The existence of the  $\Lambda(1520) \rightarrow \pi\Sigma^*(1385)$  mode and also the strength of the transition [15, 18] is a prediction of the chiral unitary models [14, 19], where the  $\pi\Sigma^*(1385)$  channel is the most important one in the dynamic coupled-channel formation of the  $\Lambda(1520)$  state.

The model diagrams describing the renormalization of the  $\Lambda(1520)$  in the nuclear medium are shown in fig. 1. As one can see, the in-medium propagation of pions in the loops is affected by the excitation of the  $p$ -hole and  $\Delta(1232)$ -hole states and in the antikaon  $\bar{K}$  case by the excitation of the all relevant hyperon-hole states. The intermediate baryons (hyperons) in the loops are also dressed with respect to their own decay channels properly renormalized in the nuclear medium. The latter includes the dressing by means of the phenomenological optical potentials which account for the nuclear binding corrections,

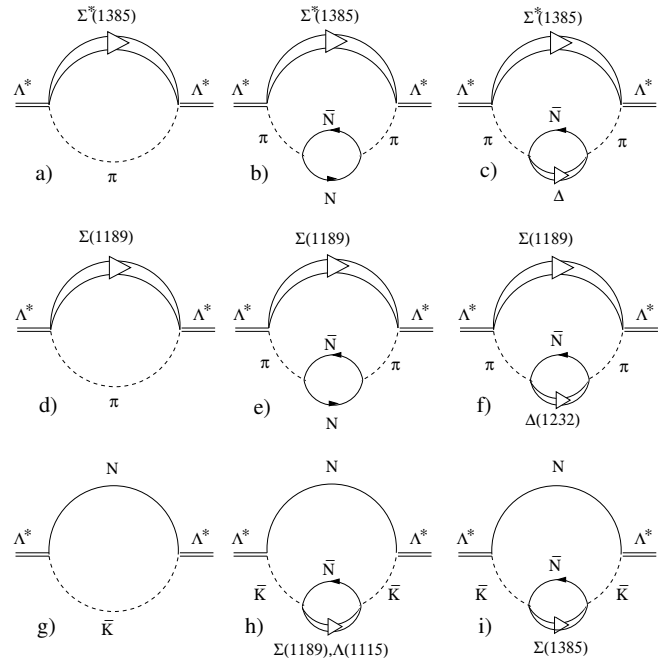


**Fig. 1.** Renormalization of the  $\Lambda(1520)$  in the nuclear medium in the  $s$ -wave  $\pi\Sigma^*(1385)$  and  $d$ -wave  $\bar{K}N$  and  $\pi\Sigma$  channels.

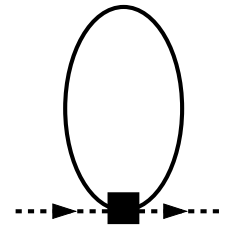


**Fig. 2.** The  $s$ -wave self-energy graph of the  $\bar{K}$  in the nuclear medium.

Pauli blocking for the nucleons and short-range correlations in the  $p$ -wave transitions induced by the strong repulsive forces at short inter-baryon distances of the Landau-Migdal type [20].

The model of ref. [16] takes into account the  $p$ -wave interaction of the  $\bar{K}$  in the  $\bar{K}N$  loops only. The corrections to the  $\bar{K}$  self-energy due to the in-medium  $s$ -wave interaction of the  $\bar{K}$  (see fig. 2) can be estimated using the formula [21]

$$\Pi_{\bar{K}}^{s-wave} = -2\omega_{\bar{K}} \left( 40 \text{ MeV} + i50 \text{ MeV} \right) \times \frac{\rho}{\rho_0}, \quad (1)$$

where  $\omega_{\bar{K}}$  is the energy of the  $\bar{K}$  and  $\rho_0 = 0.17 \text{ fm}^{-3}$  is the normal nuclear matter density. The  $s$ -wave self-energy is introduced in the calculation substituting  $m_{\bar{K}}^2$  by  $m_{\bar{K}}^2 + \Pi_{\bar{K}}^{s-wave}$  in the  $\bar{K}$  propagator. The renormalization of the  $\Lambda(1520)$  width in the  $d$ -wave  $\bar{K}N$  channel which now includes both, the  $p$ -wave and  $s$ -wave self-energies of antikaons is shown in fig. 3 (left panel). Here the solid curve is the free width in this channel. The dashed curve is the result of the  $p$ -wave interaction of the  $\bar{K}$  (from ref. [16]). The dot-dashed curve corresponds to the sum of the  $p$ - and  $s$ -wave interactions of the  $\bar{K}$  in the nuclear

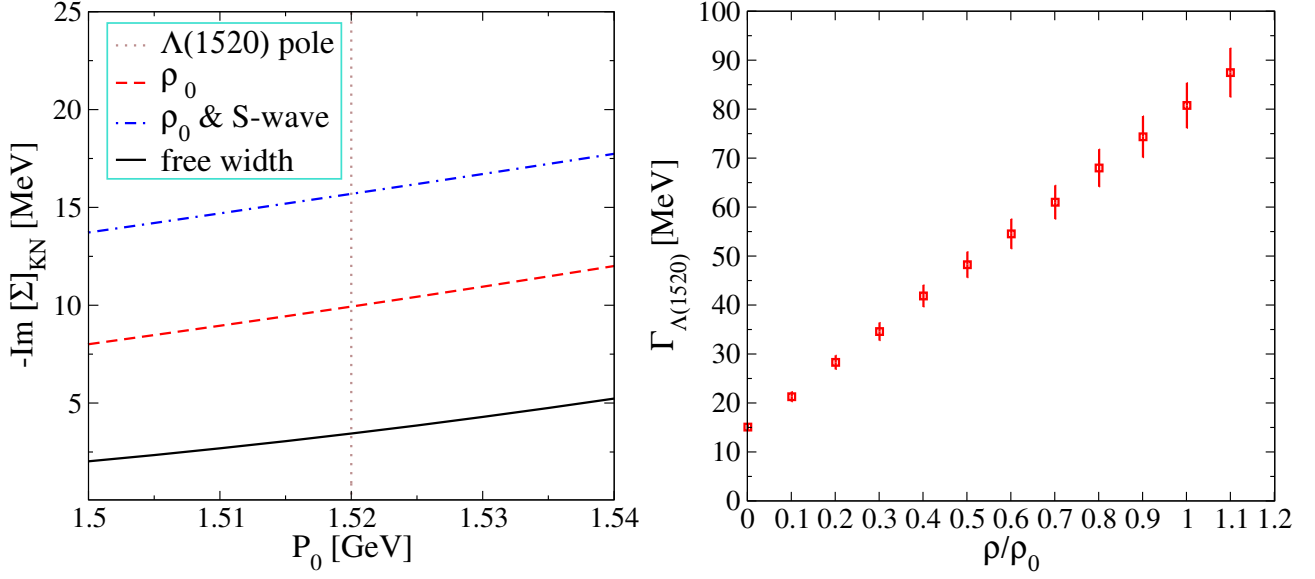


**Fig. 3.** Left panel: renormalization of the width of the  $\Lambda(1520)$  at rest  $P = (P_0, 0)$  in the  $\bar{K}N$  channel at normal nuclear-matter density. The solid curve is the free width in this channel, fig. 1(g). The dashed curve is the result of the  $p$ -wave interaction of the  $\bar{K}$  (from ref. [16]), figs. 1(h) and (i). The dot-dashed curve corresponds to the sum of the  $p$ - and  $s$ -wave interactions of the  $\bar{K}$  in the nuclear medium. Right panel: the  $\Lambda(1520)$  width in the nuclear medium as a function of the density  $\rho/\rho_0$ , where  $\rho_0$  is the normal nuclear-matter density. The error bar is explained in the text. In addition to the result obtained in ref. [16] the  $s$ -wave interaction of the  $\bar{K}$  has been taken into account, producing an increase of  $\Gamma_{\Lambda(1520)}$  of  $\simeq 14\%$  at  $\rho = \rho_0$ .

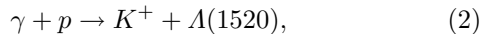
medium. From the  $s$ -wave interaction we get  $\Delta\Gamma_{\Lambda^*}^{s\text{-wave}} = -2\mathcal{I}m\Sigma_{\Lambda^*}^{s\text{-wave}} \simeq 11$  MeV, at normal nuclear matter density, in addition to the result already reported in ref. [16].

In fig. 3 (right panel) we show the model prediction for the width  $\Gamma_{\Lambda^*}$  of the  $\Lambda(1520)$  at rest and at the nominal pole position as a function of the nuclear-matter density  $\rho/\rho_0$ . The error bars reflect the theoretical uncertainties due to the choice of the momentum cut-off in the  $d$ -wave loops, with a cut-off constrained by studies of refs. [15, 18] (see other details in refs. [16, 22]). The model predicts a significant change of the width of the  $\Lambda(1520)$  in the nuclear medium which gets increased by a factor  $\sim 5$  at normal nuclear-matter densities.

In the following we address the impact of the in-medium width of the  $\Lambda(1520)$  in the  $\gamma$ - and  $p$ -induced production of this hyperon from nuclei. We shall also consider other relevant nuclear effects in the production cross-section which will be implemented here by using standard many-body techniques, successfully applied and tested in the past in many works [3, 23] to study the interaction of different particles with nuclei. A considerable simplification will be achieved by assuming a local Fermi sea at each point in the nucleus. The latter provides a very simple but accurate way to account for the Fermi motion of the initial nucleon and for the Pauli blocking of the final ones.

### 3 Nuclear effects in the $\Lambda(1520)$ photoproduction

We start with the photo-induced production of the  $\Lambda(1520)$  in nuclei. The elementary reaction will be



where we consider the photoproduction of  $K^+\Lambda(1520)$  pairs from protons only. There are several theoretical works on this reaction [24–27], but the models, as well as the couplings of the  $\Lambda(1520)$  to different channels, are rather different in all these works. However, for the purpose of the present work, the detailed dynamics of the  $\gamma p \rightarrow K^+\Lambda(1520)$  reaction is not needed since we shall evaluate ratios of cross-sections between different nuclei.

We evaluate the nuclear distortion factor due to the  $\Lambda(1520)$  absorption using the eikonal approximation, where the propagation of the  $\Lambda(1520)$  in its way out of the nucleus can be accounted for by means of the exponential factor describing the probability of loss of flux per unit length.

We proceed as follows: let  $\Sigma(p_{\Lambda^*}, \rho(r))$  be the  $\Lambda(1520)$  self-energy in the nuclear medium, calculated using the model of ref. [16], as a function of its three-momentum,  $p_{\Lambda^*}$ , and the nuclear density,  $\rho(r)$ . We have for the width

$$\Gamma = -2\mathcal{I}m\Sigma; \quad \Gamma \equiv \frac{d\mathcal{P}}{dt}, \quad (3)$$

where  $\mathcal{P}$  is the probability of  $\Lambda(1520)$  interaction in the nucleus, including  $\Lambda(1520)$  quasielastic collisions and  $\Lambda(1520)$  absorption. We shall not consider the part of the  $\mathcal{I}m\Sigma$  due to the quasielastic collisions since, even if the nucleus gets excited, the  $\Lambda(1520)$  will still be there to be observed. Thus, only the absorption of the  $\Lambda(1520)$  is reflected in the loss of  $\Lambda(1520)$  events in the nuclear production. This part of the  $\Lambda(1520)$  self-energy is the one calculated in [16]. Hence, we have for the probability of

loss of flux per unit length

$$\frac{d\mathcal{P}}{dl} = \frac{d\mathcal{P}}{v dt} = \frac{d\mathcal{P}}{\frac{|\mathbf{p}_{\Lambda^*}|}{\omega_{\Lambda^*}} dt} = -2\omega_{\Lambda^*} \frac{\mathcal{I}m\Sigma}{|\mathbf{p}_{\Lambda^*}|}, \quad (4)$$

with  $\omega_{\Lambda^*} = \sqrt{\mathbf{p}_{\Lambda^*}^2 + M_{\Lambda^*}^2}$  and the corresponding survival probability is given by

$$\exp \left[ - \int_0^\infty dl \frac{(-1)}{|\mathbf{p}_{\Lambda^*}|} 2\omega_{\Lambda^*} \mathcal{I}m\Sigma(|\mathbf{p}_{\Lambda^*}|, \rho(\mathbf{r}')) \right], \quad (5)$$

where  $\mathbf{r}' = \mathbf{r} + l \frac{\mathbf{p}_{\Lambda^*}}{|\mathbf{p}_{\Lambda^*}|}$  with  $\mathbf{r}$  being the  $\Lambda(1520)$  production point inside the nucleus. The study of the  $A$ -dependence of the total nuclear cross-section due to the  $\Lambda(1520)$  absorption, eq. (5), is the main aim of this work, since it reflects the modification of the  $\Lambda(1520)$  hyperon width in nuclear matter.

We proceed further by assuming a local Fermi sea. In this case the nuclear cross-section which takes into account the  $\Lambda(1520)$  absorption is given by

$$\begin{aligned} \sigma_{\gamma A} = & \frac{M_{\Lambda^*}}{8\pi^2 p_\gamma} \int d^3\mathbf{r} \int^{k_F(r)} \frac{d^3\mathbf{p}_N}{(2\pi)^3} \frac{1}{|\mathbf{P}|} \\ & \times \int_{M_{\Lambda^*}}^{\omega_{\Lambda^*}^{max}} d\omega_{\Lambda^*} \int_0^{2\pi} d\varphi_{\Lambda^*} \sum_{s_i} \sum_{s_f} |T|^2 \Theta(1 - A^2) \\ & \times \Theta(p_\gamma + E(\mathbf{p}_N) - \omega_{\Lambda^*}(\mathbf{p}_{\Lambda^*}) - m_K) \\ & \times \exp \left[ - \int_0^\infty dl \frac{(-1)}{|\mathbf{p}_{\Lambda^*}|} 2\omega_{\Lambda^*} \mathcal{I}m\Sigma(|\mathbf{p}_{\Lambda^*}|, \rho(\mathbf{r}')) \right], \quad (6) \end{aligned}$$

where the proton density is defined as  $2 \int \frac{d^3\mathbf{p}_N}{(2\pi)^3} \Theta(k_F(r) - |\mathbf{p}_N|) = \rho_p(r)$ , with  $\mathbf{p}_N$  the momentum of protons in the Fermi sea,  $k_F$  the Fermi momentum at the local point,  $\Theta$  the step function and  $\omega_{\Lambda^*}^{max} = p_\gamma + M_N - m_K$ . Also, in eq. (6),  $p_\gamma$  is the photon momentum in the laboratory frame (the nucleus is at rest),  $\mathbf{P} = \mathbf{p}_\gamma + \mathbf{p}_N$  is the total  $\gamma N$  three-momentum and  $A$  is defined as follows:

$$\begin{aligned} A \equiv & \frac{1}{2|\mathbf{P}||\mathbf{p}_{\Lambda^*}|} \\ & \times \left\{ \mathbf{P}^2 + \mathbf{p}_{\Lambda^*}^2 + m_K^2 - [p_\gamma + E(\mathbf{p}_N) - \omega_{\Lambda^*}(\mathbf{p}_{\Lambda^*})]^2 \right\}. \quad (7) \end{aligned}$$

The binding of the initial nucleon is accounted for by  $V_s(\mathbf{r}) = -\epsilon_F(\mathbf{r}) = -k_F^2(r)/(2M_N)$ , and in all places where we have  $E(\mathbf{p}_N)$  we put  $E(\mathbf{p}_N) = \sqrt{\mathbf{p}_N^2 + M_N^2} + V_s(\mathbf{r})$ .

For  $\mathcal{I}m\Sigma$  in the distortion factor we should take all sources contributing to the self-energy which do not go into the final detection channel. Detection of the  $\Lambda(1520)$  is done mostly by reconstruction through its  $K^-p$  decay channel, or  $\bar{K}^0 n$  channel in present set-ups at ELSA. The  $K^-p$  decay channel should be removed because one can detect it. However, the partial decay width into the  $K^-p$  is  $\simeq 3.5$  MeV only, out of which, some  $K^-$  might still be absorbed or have quasielastic collisions. This is only a very small fraction leading to an error of 5%. In view of this, and neglecting the small fraction of the  $\Lambda(1520) \rightarrow K^-p$  decay followed by  $K^-$  absorption in secondary steps, we

consider for  $\mathcal{I}m\Sigma$  in eq. (5) only the  $\Lambda(1520)$  in-medium self-energy calculated in ref. [16] subtracting the free one. Note also that there is no coherent production here since there is always conversion of an initial proton into a  $\Lambda(1520)$ , *i.e.* the nucleus does not remain in its ground state.

We shall evaluate the ratio between the nuclear cross-sections in heavy nuclei and a light one, for instance  $^{12}\text{C}$ , since in this way, many other nuclear effects not related to the distortion of the  $\Lambda(1520)$  cancel in the ratio, as was shown in ref. [11]. In the ratio of the cross-sections we shall eliminate  $|\bar{T}|^2$  which should cancel if the latter is not much energy dependent. In this respect, let us consider that the  $K^+\Lambda(1520)$  production will be measured by looking at  $d\sigma_{\gamma A}/dM_{K-p}$  and selecting the contribution of the peak of the  $K^-p$  invariant mass around the  $\Lambda(1520)$ . This gives a very restricted phase space where the cancellation of  $|\bar{T}|^2$  is justified.

In eq. (6) we have considered the  $K^+\Lambda(1520)$  production on the protons of the target. In principle, we could also have  $K^+\Lambda(1520)$  production in two-step processes like  $\gamma n \rightarrow K^0\Lambda(1520)$  followed by  $K^0 p \rightarrow K^+ n$ . The chances for this two-step reaction are not large, but in any case, one of the good things to make ratios of cross-sections on heavy nuclei to light nuclei is that the effect of these two-step processes is highly reduced in the ratio [11].

## 4 Nuclear effects in the p-induced $\Lambda(1520)$ production

In a similar way to what was obtained in ref. [11] for the  $\phi$ -meson production in the  $p$ -induced reaction, we expect the  $A$ -dependence of the  $pA \rightarrow A'K^+\Lambda(1520)$  reaction in nuclei to provide also a conclusive test of the modification of the  $\Lambda(1520)$  width in the nuclear medium. Within the local Fermi sea approach the  $pA$  nuclear cross-section can be evaluated, as a first approximation, as

$$\sigma_{pA}(p_{Lab}) = 4 \int d^3\mathbf{r} \int \frac{d^3\mathbf{k}}{(2\pi)^3} \Theta(k_F - |\mathbf{k}|) \sigma_m(p_{Lab}, \mathbf{k}, \mathbf{r}), \quad (8)$$

where  $p_{Lab}$  is the momentum of the incident proton and  $\sigma_m$  the elementary  $pp \rightarrow pK^+\Lambda(1520)$ ,  $pn \rightarrow nK^+\Lambda(1520)$  average cross-section in the nuclear medium, which will be defined later in eq. (10).

One of the main differences of the  $p$ -induced reaction with respect to the photoproduction case previously discussed is the fact that the incident proton is strongly distorted in its way to the reaction point. This effect can be properly considered by adding in eq. (8) the following eikonal factor:

$$\exp \left[ - \int_{-\infty}^z \sigma_{pN}(p_{Lab}) \rho(\sqrt{b^2 + z'^2}) dz' \right], \quad (9)$$

where  $z$  and  $b$  are the position in the beam axis and the impact parameter, respectively, of the production point  $\mathbf{r}$  of eq. (8). In eq. (9)  $\sigma_{pN}$  is the total  $pp$  and  $pn$  averaged experimental cross-section, taken from [17], for a given

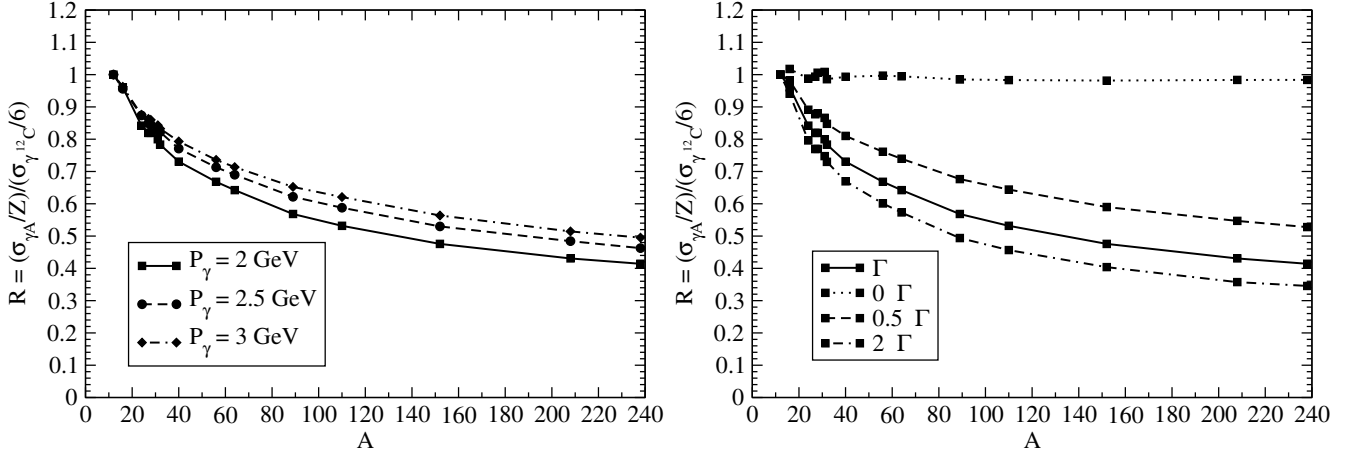


**Fig. 4.** The nuclear cross-section for the  $\gamma$ -induced production of the  $\Lambda(1520)$ . Left panel:  $\sigma_{\gamma A}/Z$  for different nuclei normalized to the same fraction of  $^{12}\text{C}$  for  $p_\gamma = 2, 2.5$  and  $3$  GeV. Right panel: the same for  $p_\gamma = 2$  GeV and multiplying the in-medium width of the  $\Lambda(1520)$  by different factors.

incident proton momentum. Equation (9) represents the probability for the proton to reach the reaction point without having a collision with the nucleons, since  $\sigma_{pN}\rho$  is the probability of proton collisions per unit length. There is of course the possibility of having the reaction through two-step collisions, but this was discussed in [11] and found to cancel to a great extent in the ratios of cross-sections of heavy to medium nuclei.

The elementary cross-section in the nuclear medium for the  $p(p_{Lab}) + N(k) \rightarrow N(p_1) + K^+(p_2) + \Lambda^*(p_{A^*})$  reaction is

$$\begin{aligned} \sigma_m(p_{Lab}, \mathbf{k}, \mathbf{r}) &\sim \frac{1}{|\mathbf{p}_{Lab}|} \\ &\times \int d\Omega_{A^*} \int d|\mathbf{p}_{A^*}| \mathbf{p}_{A^*}^2 \int d|\mathbf{p}_1| \frac{|\mathbf{p}_1|}{|\mathbf{P}|} \frac{1}{E(\mathbf{p}_1) \omega_{A^*}(\mathbf{p}_{A^*})} \\ &\times \overline{\sum_{s_i} \sum_{s_f} |T|^2 \Theta(1 - B^2) \Theta(|\mathbf{p}_1| - k_F(r)) \Theta(|\mathbf{p}_2| - k_F(r))} \\ &\times \Theta(E(\mathbf{p}_{Lab}) + E(\mathbf{k}) - E(\mathbf{p}_1) - \omega_{A^*}(\mathbf{p}_{A^*}) - m_K) \end{aligned} \quad (10)$$

up to some global constants irrelevant in the final results since they will cancel when we will evaluate the ratio of different nuclei to  $^{12}\text{C}$ . In eq. (10)  $\mathbf{P} = \mathbf{p}_{Lab} + \mathbf{k} - \mathbf{p}_{A^*}$ , and  $B$  provides the cosine of the angle between  $\mathbf{P}$  and  $\mathbf{p}_1$ ,

$$\begin{aligned} B \equiv \frac{1}{2|\mathbf{P}||\mathbf{p}_1|} &\left\{ m_K^2 + \mathbf{P}^2 + \mathbf{p}_1^2 - [E(\mathbf{p}_{Lab}) \right. \\ &\left. + E(\mathbf{k}) - E(\mathbf{p}_1) - \omega_{A^*}(\mathbf{p}_{A^*})]^2 \right\}, \end{aligned}$$

with  $E(\mathbf{q}) = \sqrt{M_N^2 + \mathbf{q}^2}$ ,  $\omega_{A^*}(\mathbf{p}_{A^*}) = \sqrt{M_{A^*}^2 + \mathbf{p}_{A^*}^2}$ . In eq. (10) the azimuthal angle of  $\mathbf{p}_1$  with respect to  $\mathbf{P}$  has already been integrated, assuming that  $|T|^2$  does not depend on this angle.

Gathering all these results, the final expression for the  $\Lambda^*$  production cross-section in nuclei reads, up to a global

constant factor,

$$\begin{aligned} \sigma_A(p_{Lab}) &\sim \frac{1}{|\mathbf{p}_{Lab}|} \\ &\times \int d^2b \int_{-\infty}^{\infty} dz \exp \left\{ - \int_{-\infty}^z \sigma_{pN}(p_{Lab}) \rho(\sqrt{b^2 + z'^2}) dz' \right\} \\ &\times \int d^3\mathbf{k} \int d|\mathbf{p}_1| \int d\Omega_{A^*} \int d|\mathbf{p}_{A^*}| \frac{\mathbf{p}_{A^*}^2 |\mathbf{p}_1|}{|\mathbf{P}| E(\mathbf{p}_1) \omega_{A^*}(\mathbf{p}_{A^*})} \\ &\times \overline{\sum_{s_i} \sum_{s_f} |T|^2 \Theta(1 - B^2)} \\ &\times \Theta(k_F - |\mathbf{k}|) \Theta(|\mathbf{p}_1| - k_F(r)) \Theta(|\mathbf{p}_2| - k_F(r)) \\ &\times \Theta(E(\mathbf{p}_{Lab}) + E(\mathbf{k}) - E(\mathbf{p}_1) - \omega_{A^*}(\mathbf{p}_{A^*}) - m_K) \\ &\times \exp \left\{ - \int_0^{\infty} dl \frac{(-1)}{|\mathbf{p}_{A^*}|} 2\omega_{A^*} \mathcal{I}m\Sigma(|\mathbf{p}_{A^*}|, \rho(\mathbf{r}')) \right\}. \end{aligned} \quad (11)$$

## 5 Results and discussion

We performed calculations for the following nuclei:  $^{12}\text{C}$ ,  $^{16}\text{O}$ ,  $^{24}\text{Mg}$ ,  $^{27}\text{Al}$ ,  $^{28}\text{Si}$ ,  $^{31}\text{P}$ ,  $^{32}\text{S}$ ,  $^{40}\text{Ca}$ ,  $^{56}\text{Fe}$ ,  $^{64}\text{Cu}$ ,  $^{89}\text{Y}$ ,  $^{110}\text{Cd}$ ,  $^{152}\text{Sm}$ ,  $^{208}\text{Pb}$ ,  $^{238}\text{U}$ .

In fig. 4 (left panel) we present our results for the ratio of the nuclear cross-sections normalized to  $^{12}\text{C}$  as a function of the mass number  $A$ . The curves correspond to the incident  $\gamma$  momenta in the laboratory frame  $p_\gamma = 2$  (solid line),  $2.5$  (dashed line) and  $3$  GeV (dot-dashed line). Recall that, contrary to the  $p$ -induced production, in the  $\gamma$ -induced reaction the elementary cross-section is defined with respect to the protons in the Fermi sea only. Hence, the nuclear cross-sections are normalized to the number of protons  $Z$  in the corresponding nucleus,  $(\sigma_{\gamma A}/Z)$ .

As one can see, we obtain a significant reduction of flux relative to  $^{12}\text{C}$  which can reach the value  $\simeq 0.4$ – $0.5$  for heavy nuclei. It is also instructive to renormalize artificially the model prediction for the  $\Lambda(1520)$  self-energy

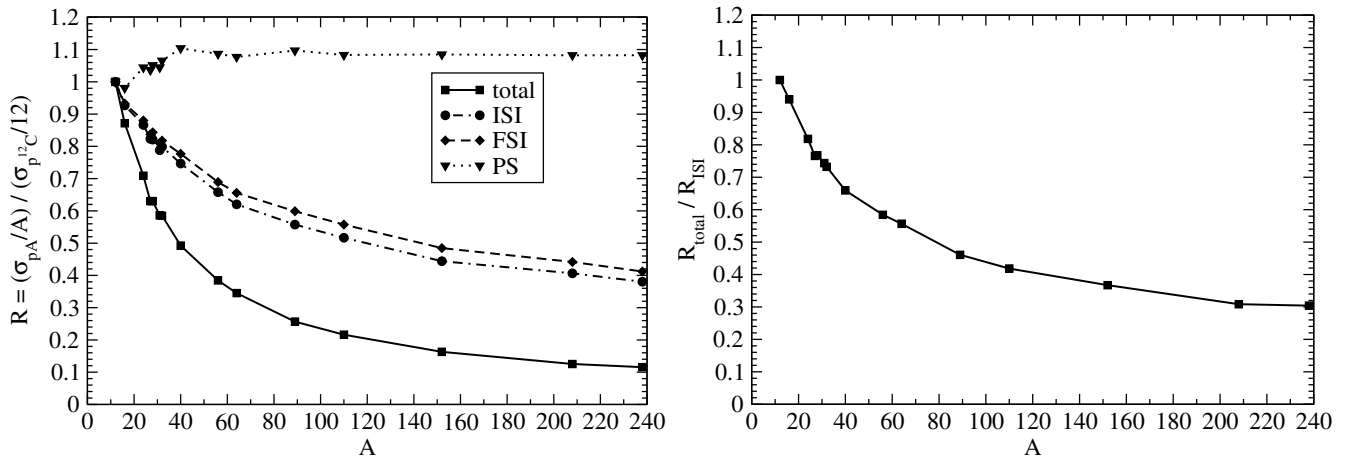


**Fig. 5.** The nuclear cross-section for the  $p$ -induced production of the  $\Lambda(1520)$  in different nuclei. Left panel: the fraction  $\sigma_{pA}/A$  as a function of the mass number  $A$  normalized to that of  $^{12}\text{C}$  for the proton kinetic energy  $T_p = 2.9$  GeV. The different lines correspond to the consideration of the phase space (PS), the initial-state interaction (ISI), the final-state interaction (FSI) and the total cross-section. Right panel: ratio of the total result to ISI for  $T_p = 2.9$  GeV.

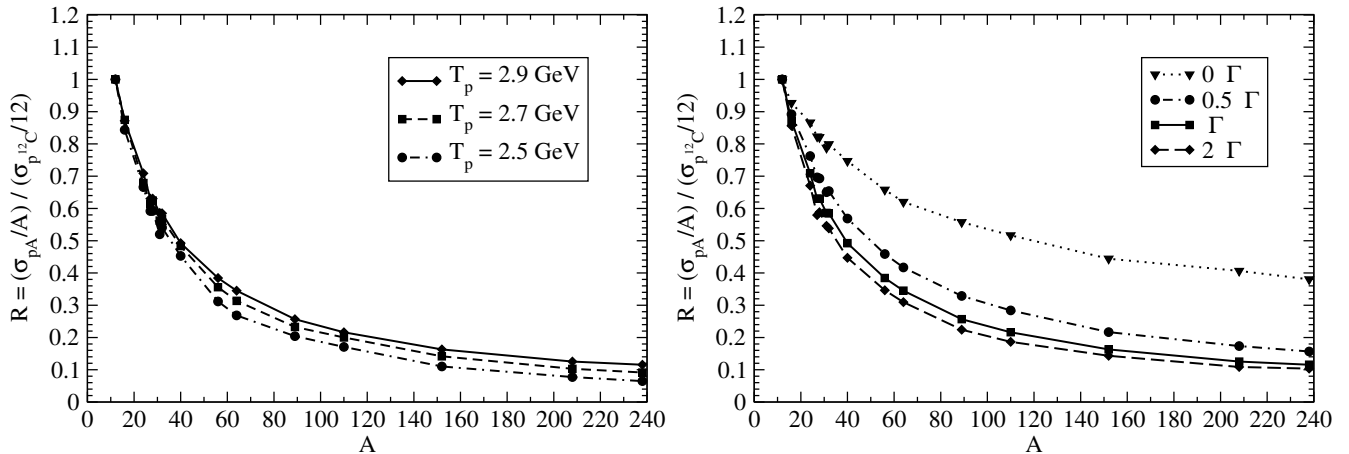


**Fig. 6.** Left panel: ratio of the nuclear cross-section normalized to  $^{12}\text{C}$  for  $T_p = 2.5$  (dot-dashed line),  $2.7$  (dashed line) and  $2.9$  GeV (solid line). Right panel: ratio of the nuclear cross-section normalized to  $^{12}\text{C}$  for  $T_p = 2.9$  GeV multiplying the  $\Lambda(1520)$  width in the medium by different factors.

by some factors and look on the corresponding ratio of the nuclear cross-sections. In fig. 4 (right panel) we show our results for  $f \cdot \mathcal{I}m\Sigma$  entering the eikonal factor, where the factor  $f$  is taken as  $f = 0, 0.5, 1$  and  $2$ . The calculations are performed for  $p_\gamma = 2$  GeV. These results are instructive because they tell us with which accuracy the ratios must be measured experimentally to induce a certain value of the  $\Lambda(1520)$  in-medium width.

Next, we present the results for the  $p$ -induced production. In fig. 5 (left panel) we show  $(\sigma_A/A)$  normalized to the value for  $^{12}\text{C}$  as a function of the mass number and for a projectile energy of  $T_p = 2.9$  GeV. The different lines correspond to the consideration of the phase space (PS) alone, eq. (8); phase space and initial-state interaction, eq. (8), including the distortion factor of eq. (9) (ISI); phase space and final-state interaction, eq. (8), including the distortion factor of eq. (5) (FSI); and complete cal-

culcation (total), *i.e.* the simultaneous consideration of all the effects, eq. (11).

As we can see in the figure, the PS curve is quite stable with respect to  $A$ , almost saturating from about  $A \sim 50$  on. This feature is common for both,  $p$ -induced and  $\gamma$ -induced productions. This is just a consequence of the density profiles of the different nuclei which makes that the average density of each nuclei almost saturates with  $A$ . By looking at the dot-dashed line, the effect of the distortion of the incident proton in its way through the nucleus is significant. This is the most important difference of the production induced by protons with respect to the photoproduction case. The dashed line represents the effect of only considering the FSI of the  $\Lambda(1520)$ , but not the ISI. The difference of this curve to the PS curve is only due to the modification of the  $\Lambda(1520)$  in the medium. The solid line represents the calculation obtained including all the effects considered. Now if we look at ISI and

FSI curves, we see that in both cases there is a sizeable decrease of the observable, particularly for ISI, which shows a stronger  $A$ -dependence. Although the ISI and “total” curves are almost parallel, the absolute values decrease with  $A$  and therefore the contribution of the FSI becomes more and more important. This significant  $A$ -dependence can be seen in the ratio of these two curves which is shown in fig. 5 (right panel). This is also in agreement with what we find for photoproduction, where there is no initial-state distortion. From this figure we can conclude that in the  $A$ -dependence there is indeed valuable information concerning the  $\Lambda(1520)$  absorption and hence, the  $\Lambda(1520)$  width in the medium, which is the main conclusion of the present work.

The total result including all the many-body effects discussed above, but for other projectile energies with  $T_p = 2.7$  and  $2.5$  GeV, is shown in fig. 6 (left panel). Also in fig. 6 (right panel) we show the total results for  $T_p = 2.9$  GeV but multiplying artificially the  $\Lambda(1520)$  self-energy by different factors in order to check the sensitivity of the observable to the value of the width. This curves could serve to get a fair answer about the  $\Lambda(1520)$  width in the medium by comparing with experimental results.

## 6 Summary

In summary, we have discussed the mass dependence of the  $\gamma$ - and  $p$ -induced production of the  $\Lambda(1520)$  hyperons from nuclei. The main motivation for this study is a prediction of the spectacular increase of the width of the  $\Lambda(1520)$  in the nuclear medium which can reach the factor  $\sim 5$  at normal nuclear-matter density. Indications that this might be the case can be seen in the analysis of  $\Lambda(1520)$  production in heavy-ion reactions [28, 29].

We have shown that both reactions, the  $\gamma$ - and  $p$ -induced  $\Lambda(1520)$  production can provide an interesting tool to investigate the properties of the  $\Lambda(1520)$  hyperon and particularly the modification of its width in the nuclear medium. The calculations presented here predict a considerable reduction of flux of the  $\Lambda(1520)$  in heavy nuclei with respect to light ones. We have also shown that the opening of the in-medium absorption channels and associated increase of the width of the  $\Lambda(1520)$  with increasing nuclear-matter density is a large source of such reduction in the proton-induced production and practically the only one in the case of photoproduction. These effects are significant, and devoted experiments, easily within reach in present facilities like Spring 8, ELSA and COSY, can provide good information on that magnitude, by measuring the cross-sections studied here.

## References

1. P. Carlos, H. Beil, R. Bergere, J. Fagot, A. Lepretre, A. de Miniac, A. Veyssiere, Nucl. Phys. A **431**, 573 (1984).
2. E. Oset, L.L. Salcedo, Nucl. Phys. A **468**, 631 (1987).
3. R.C. Carrasco, E. Oset, Nucl. Phys. A **536**, 445 (1992).
4. F. Klingl, T. Waas, W. Weise, Phys. Lett. B **431**, 254 (1998) [arXiv:hep-ph/9709210].
5. E. Oset, A. Ramos, Nucl. Phys. A **679**, 616 (2001) [arXiv:nucl-th/0005046].
6. D. Cabrera, M.J. Vicente Vacas, Phys. Rev. C **67**, 045203 (2003) [arXiv:nucl-th/0205075].
7. E. Oset, M.J. Vicente Vacas, H. Toki, A. Ramos, Phys. Lett. B **508**, 237 (2001) [arXiv:nucl-th/0011019].
8. P. Muhlich, T. Falter, C. Greiner, J. Lehr, M. Post, U. Mosel, Phys. Rev. C **67**, 024605 (2003) [arXiv:nucl-th/0210079].
9. T. Ishikawa *et al.*, Phys. Lett. B **608**, 215 (2005).
10. D. Cabrera, L. Roca, E. Oset, H. Toki, M.J. Vicente Vacas, Nucl. Phys. A **733**, 130 (2004) [arXiv:nucl-th/0310054].
11. V.K. Magas, L. Roca, E. Oset, Phys. Rev. C **71**, 065202 (2005) [arXiv:nucl-th/0403067].
12. M. Hartmann *et al.*, Experiment 147.
13. S. Sarkar, E. Oset, M.J. Vicente Vacas, Phys. Rev. C **72**, 015206 (2005) [arXiv:hep-ph/0503066].
14. E.E. Kolomeitsev, M.F.M. Lutz, Phys. Lett. B **585**, 243 (2004).
15. L. Roca, S. Sarkar, V.K. Magas, E. Oset, Phys. Rev. C **73**, 045208 (2006) [arXiv:hep-ph/0603222].
16. M. Kaskulov, E. Oset, Phys. Rev. C **73**, 045213 (2006) [arXiv:nucl-th/0509088].
17. Particle Data Group Collaboration (K. Hagiwara *et al.*), Phys. Rev. D **66**, 010001 (2002).
18. S. Sarkar, L. Roca, E. Oset, V.K. Magas, M.J.V. Vacas, arXiv:nucl-th/0511062.
19. S. Sarkar, E. Oset, M.J. Vicente Vacas, Nucl. Phys. A **750**, 294 (2005).
20. M.M. Kaskulov, E. Oset, M.J. Vicente Vacas, Phys. Rev. C **73**, 014004 (2006); [arXiv:nucl-th/0506031].
21. A. Ramos, E. Oset, Nucl. Phys. A **671**, 481 (2000).
22. M.M. Kaskulov, E. Oset, arXiv:nucl-th/0512108.
23. L.L. Salcedo, E. Oset, M.J. Vicente-Vacas, C. Garcia-Recio, Nucl. Phys. A **484**, 557 (1988).
24. L. Roca, E. Oset, H. Toki, arXiv:hep-ph/0411155.
25. A. Sibirtsev, J. Haidenbauer, S. Krewald, U.G. Meissner, A.W. Thomas, arXiv:hep-ph/0509145.
26. S.I. Nam, A. Hosaka, H.C. Kim, Phys. Rev. D **71**, 114012 (2005) [arXiv:hep-ph/0503149].
27. A.I. Titov, B. Kampfer, S. Date, Y. Ohashi, Phys. Rev. C **72**, 035206; 049901 (2005)(E) [arXiv:nucl-th/0506072].
28. J. Rafelski, J. Letessier, G. Torrieri, Phys. Rev. C **64**, 054907 (2001); **65**, 069902 (2002)(E) [arXiv:nucl-th/0104042].
29. C. Markert, G. Torrieri, J. Rafelski, arXiv:hep-ph/0206260.